FINGERPRINT IMAGE ENHANCEMENT USING WAVELET TRANSFORM AND GABOR FILTERING

Vipan KAKKAR, Abhishek SHARMA, T.K. MANGALAM, Pallavi KAR
School of Electronics & Comm. Engg. SMVD University,
Sub Post Office, Katra, vipan.kakar@smvdu.ac.in

Abstract Automatic Fingerprint Identification System (AFIS) have become the most widely and popular technology in rapidly growing bio-identification applications. Fingerprint identification consists of various stages viz. image acquisition, enhancement, feature extraction and matching. The performance of a fingerprint recognition system highly relies on the quality of the fingerprint images. The enhancement is an essential step required to improve the quality of the fingerprint image. In this paper, we propose a enhancement method based on gabor filtering in wavelet domain. Gabor filter is so chosen because it has both frequency-selective and orientation-selective properties and has optimal resolution in both spatial and frequency domain. Filtering is done on the images results from wavelet decomposition and finally, the image is reconstructed to get the enhanced image. Experiments are conducted on 500dpi resolution fingerprint images commercially available from FVC2002 fingerprint database.

Keywords*: Fingerprint Identification, Image Enhancement, Gabor Filter, Wavelet Transform.*

I. INTRODUCTION

The term biometric recognition or simply biometrics refers to the use of various characteristic called biometric identifier or trait for automatically recognizing the individual [1]. The characteristic can be physiological i.e. related to the shape of the body (e.g. face, fingerprint, hand and palm geometry etc.) or behavioural i.e. related to the behavior of a person (e.g. gait, voice etc.).

The most popular and widely used bio-identification system is fingerprint recognition system because of the fact that fingerprints of human are unique and persistent. Fingerprints of even identical twins are different. A fingerprint can be seen as smoothly varying pattern formed by alternating crest (ridges) and troughs (valleys) on the surface of the finger as shown in Fig. 1. The ridges are the dark lines and valleys are the light lines in the fingerprint image pattern. The various types of fingerprints are shown in Fig. 2.

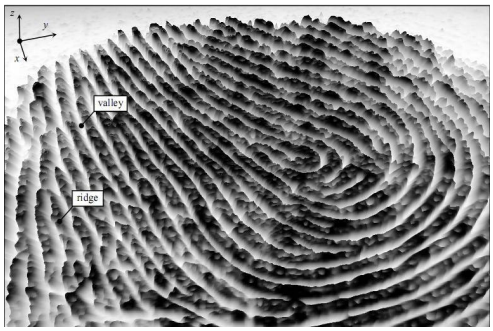

Figure 1. Ridge and Valley Structure [1].

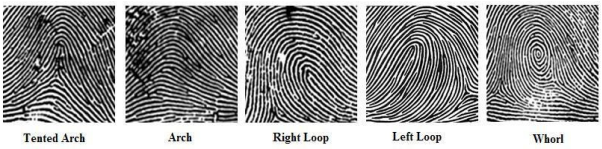

Figure 2. Types of Fingerprints [1].

Most of the automatic fingerprint identification system (AFIS) are based on the minutiae matching. Minutiae or Galton's characteristic [2] are the local discontinuities in the fingerprint pattern. The American National Standards Institute [3] has proposed a minutiae classification based on four classes : terminations, bifurcations, trifurcations (or crossover) and undetermined. The various types of minutiae are shown in Fig. 3.

Prior to feature extraction and matching the the clarity of ridges and valleys of the fingerprint image should be improve to make them more suitable for the minutiae extraction algorithm. local features i.e. minutiae can be extracted easily for the matching purpose. There have existed many research on fingerprint image enhancement algorithm. Hong et al [4], [5] and Greenberg et al [6] has suggested a filter based method of enhancement. A.K. Jain et al has published several research papers on for fingerprint image enhancement [4], [5], [7]. A comparative study on fingerprint image enhancement method is done by A M Paul et al [8]. Various methods based on gabor filtering has also been proposed [9]- [12] for fingerprint image enhancement. Safar Hatami et al [13] has proposed a wavelet based method for enhancement. The various fingerprint

Manuscript received September 05, 2011; revised November 28, 2011

enhancement method suggested by various researchers can be found in [14].

In this paper, we have proposed a enhancement method based on gabor filtering in wavelet domain. The ridges and valleys in the fingerprint pattern form a sinusoidal

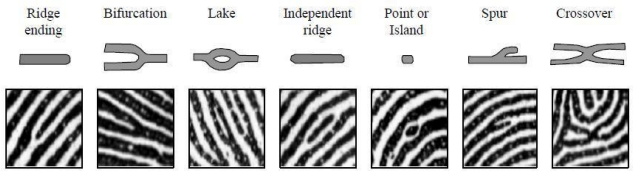

Figure 3. Various Types of Minutiae [1].

shaped plane wave with constant local orientation and frequency. Since, gabor filter has both frequency-selective and orientaion-selective properties and has optimal resolution in both spatial and frequency domain therefore we have chosen it for filtering the fingerprint image. Gabor filtering is done on the image results from wavelet decomposition and enhanced image is obtained by wavelet reconstruction.

The rest of the paper is organized as follows. Section II presents an overview of wavelet transform. Section III describes the enhancement algorithm. Experimental results and conclusion is presented in Section IV and Section V respectively.

II. WAVELET TRANSFORM: A REVIEW

The wavelet transform provides the time-frequency representation of signal. Wavelet transform is based on small waves known as wavelets of varying frequency and limited duration. Temporal information is not lost in transformation process as it is lost in fourier transformation process. Wavelet bases are constructed from translation and scale of a mother wavelet as described by the Eq. 1 [15]:

$$\psi_{a,b}(t) = \frac{1}{\sqrt{a}}\psi(\frac{t-b}{a}) \tag{1}$$

where *a* and *b* are the scaling and translation parameters,

respectively. Wavelet transform of a function $f(t) \in L^2$ is

defined as (Eq. 2),

$$Wf(a,b) = \langle f, \psi_{(a,b)} \rangle = \int_{-\infty}^{+\infty} f(x)\frac{1}{\sqrt{a}}\psi(\frac{t-b}{a})dt \tag{2}$$

The reconstruction relation can be expressed as (Eq. 3):

$$f = \frac{1}{C_\psi}\int_0^\infty \int_{-\infty}^{+\infty} Wf(a,b)\psi_{(a,b)}(t)db\frac{da}{a^2} \tag{3}$$

where, C_ψ known as Admissibility constant is defined by Eq. 4,

$$C_\psi = \int_0^\infty \frac{|\hat{\psi}(\omega)|^2}{\omega}d\omega < +\infty \tag{4}$$

where, $\psi(\omega)$ is the fourier transform of $\psi(t)$.

Wavelet transform is best suited for localized frequency analysis, because the wavelet basis function have short-time resolution for high frequencies and long-time resolution for low frequencies. It can be used to analyze the signal or image at different scale i.e. the multiresolution analysis which provides the information about the signal at more than one resolution.

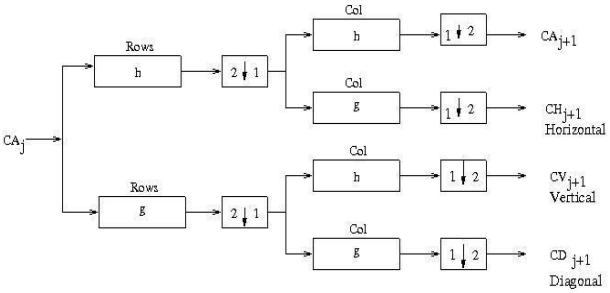

Figure 4. 2D Wavelet Decomposition.

In two dimensions, a two-dimensional scaling function, $\varphi(x, y)$ and three two-dimensional wavelet functions, $\psi^H(x, y)$, $\psi^V(x, y)$, $\psi^D(x, y)$ are required. The two-dimensional scaling and wavelet functions are described by the following equations (Eq. 5-Eq. 8),

$$\phi(x,y) = \phi(x)\phi(y) \tag{5}$$

$$\psi^H(x,y) = \psi(x)\phi(y) \tag{6}$$

$$\psi^V(x,y) = \psi(y)\phi(x) \tag{7}$$

$$\psi^D(x,y) = \psi(x)\psi(y) \tag{8}$$

These wavelets measures functional variations-intensity variations for images-along three different directions viz. horizontal, vertical and diagonal. The scaled and translated basis functions are defined as (Eq. 9-Eq. 10):

$$\phi_{j,m,n}(x,y) = 2^{\frac{j}{2}}\phi(2^j x - m, 2^j y - n) \tag{9}$$

$$\psi^i_{j,m,n}(x,y) = 2^{\frac{j}{2}}\psi^i(2^i x - m, 2^j y - n) \tag{10}$$

where index $i = H, V, D$ identifies the directional wavelets in Eq. 6 to Eq. 8. The discrete wavelet transform of image f(x, y) of size M×N is then expressed as follows:

$$W_\phi(j_0,m,n)=\frac{1}{\sqrt{MN}}\sum_{x=0}^{M-1}\sum_{y=0}^{N-1}f(x,y)\phi_{j_0,m,n}(x,y) \quad (11)$$

$$W_\psi^i(j,m,n)=\frac{1}{\sqrt{MN}}\sum_{x=0}^{M-1}\sum_{y=0}^{N-1}f(x,y)\psi_{j,m,n}^i(x,y) \quad (12)$$

where $i = H, V, D$.

Wavelet analysis can be considered to be a time-scale method embedded with the characteristic of frequency. It gives its best performance when it is applied to the detection of short time phenomena, discontinuities, or abrupt changes in signal. The decomposition of the input signal into approximation and detail space is called multi-resolution approximation, which can be realized by using a pair of finite impulse response (FIR) filters h and g, which are low-pass and high-pass filters, respectively as shown in Fig. 4. The analytical description and details regarding the wavelets can be found in Refs. [15], [16].

III. FINGERPRINT IMAGE ENHANCEMENT

Fingerprint image enhancement is of great importance as it influences the performance of subsequent feature extraction and matching process. The quality of ridge structures in the fingerprint image is an important characteristic as the ridges carry the information of characteristic features required for minutiae extraction. Ideally, in fingerprint image ridges and valleys form the sinusoidal shaped plane wave structure and flow in a locally constant direction. This regularity facilitates the detection of ridges and consequently allows minutiae to be extracted from thinned image.

This section provides discussion on the methodology and implementation of fingerprint image enhancement algorithm. Following are the steps involved in enhancement process.

A. Segmentation

Segmentation is used to separate the foreground and background area. The foreground is the component that originats from the contact of a fingertip with the sensor, whereas noisy area of the borders of the image is known as the background. The foreground area in the fingerprint contains the information and is sometimes called the Region of Interest (ROI). Some of the most important methods for fingerprint segmentation can be found in the literature [18]. In our algorithm, we have used the variance and mean based threshold method.

1) Mean and Variance of the fingerprint image: Let a gray-level image I be defined as $N \times N$ matrix where, $I(i, j)$ represents the intensity of the pixel at the ith row and jth column. Mean of the image is defined as:

$$M(I)=\frac{1}{N^2}\sum_{i=0}^{N-1}\sum_{j=0}^{N-1}I(i,j) \quad (13)$$

and the variance is defined as:

$$V(I)=\frac{1}{N^2}\sum_{i=0}^{N-1}\sum_{j=0}^{N-1}(I(i,j)-M(I))^2 \quad (14)$$

Steps involved in segmentation process:

i) Divide the input image $I(i, j)$ into the blocks of size w × w(8 × 8).
ii) Compute the mean of the image using Eq. 13.
iii) Using mean from above step, calculate the standard deviation, (std) using Eq. 15:

$$std(I)=\sqrt{V(I)} \quad (15)$$

where variance, V(I) is calculated using Eq. 14.

iv) Now, select a threshold value (thr) empirically working on different images. The threshold range comes out to be 0.1-0.2. For our experiment, we have used thr=0.2
v) If the $std(I)>thr$, then block is considered as foreground, otherwise background.

The original image and segmentated image are shown in Fig. 5 and Fig. 6, respectively.

Figure 5. Original Image.

Figure 6. Segmented Image.

B. Normalization

Normalization is done to reduce the differences in the gray-level values along the ridges and valleys so that the pixel values in the image have a specified mean and variance. Normalization is the linear and pixel-wise process

and doesn't change the ridge and valley structure. The normalized image *N(i, j)* is defined by the Eq. 16:

$$N(i,j) = \begin{cases} M_0 + \sqrt{\frac{V_0(I(i,j)-M)^2}{V}} & : \quad I(i,j) > M \\ M_0 - \sqrt{\frac{V_0(I(i,j)-M)^2}{V}} & : \quad otherwise \end{cases} \qquad (16)$$

where, *M0* and *V0* are the expected mean and variance values. Hong et al [5] have taken *M0 = 100* and *V0 = 100* for the normalization process. But, in our experiment, we have set *M0 = 0* and *V0 = 1* so that new intensities of the pixel for the normalized image would mostly be between -1 and 1, making the subsequent calculations easier. Fig. 7 shows the normalized image for the segmented image as an input.

Figure 7. Normalized Image.

C. Wavelet Decomposition

Wavelet transform can be used to decompose the signal (or image) into a multiresolution representation. The input signal (or image) can be decomposed recursively until the coarsest resolution has been achieved [17]. The convolution of signal (or image) with different base function $\psi(t)$ causes different effects in the resolution.

In our algorithm, we decompose the image only upto one level as too low resolution is not suitable because an excessive down sampling can destroy the characteristic of the ridge structure. The Haar wavelet [15] is used here, as base function for the decomposition of the image.

The two-dimensional wavelet decomposition at J level of a discrete image I(i, j) represents the image in terms of 3J + 1 sub-images as described below:

$$[a_m, (d_m^1, d_m^2, d_m^3)_{m=0,1,\ldots J}]$$

where, a_m represents low resolution approximation of the image or approximation sub-image and $d^k m$ are the sub-images containing image details at different scale and orientation. For, level 1 decomposition m = 1 and k = 3.

In our algorithm, the normalized is decomposed at level 1. Level 1 decomposition leads to one approximation sub-image and three detailed sub-images as shown in Fig. 8. Since, approximated sub-image *A(i, j)* shown in Fig. 9 and the original image shown in Fig. 5 have similar statistical information and fewer noise than original one, therefore, it is used to compute the ridge field orientation and frequency. Also, due to this the effect of over/under inking can be restrained. After level 1 decomposition the image size becomes *N/2* x *N/2*.

D. Ridge Orientation Estimation

The orientation image, *O* is defined as an *N* × *N* image where *O(i, j)* represents the local ridge orientation at the pixel *(i,j)* [5]. Local ridge orientation is usually specified for a block rather than for a pixel.

The simplest approach for extracting local ridge orientation is based on computation of gradients of the fingerprint image [1]. The gradient $\nabla(x, y)$ of an image *I(i, j)* is a two-dimensional vector $[\nabla x(x, y), \nabla y(x, y)]$,where ∇x and ∇y components are the derivative of I at *(x, y)* with respect to the x and y directions. There are many approaches for estimating the local ridge orientation [1], e.g. gradient-based approaches, slit- and projection-based approaches, orientation calculation in frequency domain etc.

In this paper, we have used simple approach i.e. the gradient-based approach. The algorithm for estimation of local ridge orientation is as follows:

1) Divide the image into a block size of *w* × *w(8* × *8).*

2) Now, the gradient of each pixel is computed using the 5 × 5 canny mask (derivative of Gaussian filter) which is convolved with the approximated image *A(i, j)* to get the gradients in x and y directions.

3) The dominant ridge orientation θ_{ij} is calculated by combining multiple gradient estimates within a window *w* centered at the pixel (x_i, y_j) by using Eq. 17,

$$\theta_{ij} = \frac{\pi}{2} + \frac{1}{2}\tan 2(2\nabla_{xy}, \nabla_{xx} - \nabla_{yy}) \qquad (17)$$

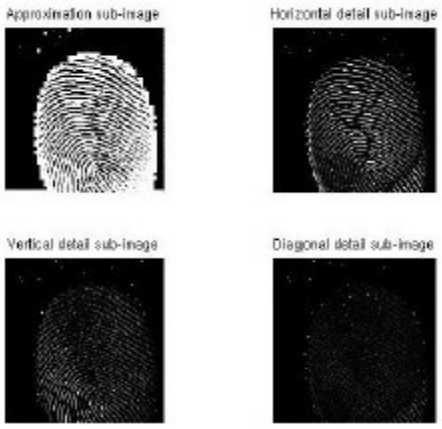

Figure 8. Level 1 Decomposition of Image.

Figure 9. Approximation Sub-Image.

where, ∇xy, ∇xx and ∇yy are defined by the following relations:

$$\nabla_{xy} = \sum_{h=-4}^{4} \sum_{k=-4}^{4} \nabla_x(x_i+h, y_j+k)\nabla_y(x_i+h, y_j+k) \quad (18)$$

$$\nabla_{xx} = \sum_{h=-4}^{4} \sum_{k=-4}^{4} \nabla_x(x_i+h, y_j+k)^2 \quad (19)$$

$$\nabla_{yy} = \sum_{h=-4}^{4} \sum_{k=-4}^{4} \nabla_y(x_i+h, y_j+k)^2 \quad (20)$$

where, ∇_x and ∇_y are the x- and y- gradient components computed through 5 × 5 canny mask.

Due to the presence of noise, corrupted ridge and valley structure, local discontinuities etc. in the image may lead to inaccurate calculation of local ridge orientation. Therefore, a Gaussian low pass filter is applied to the local ridge orientation θ_{ij}. In order to perform filtering, the oriented image needs to be converted into a continuous vector field defined by the Eq. 21 and Eq. 22 [5]:

$$\Phi_x(i,j) = \cos(2\theta_{ij}) \quad (21)$$

$$\Phi_y(i,j) = \sin(2\theta_{ij}) \quad (22)$$

where, Φx and Φy are the x and y components of the vector field.

Figure 10. Orientation Field plot with image overlapping.

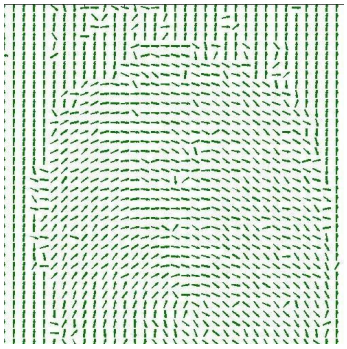

Figure 11. Orientation Field plot without image overlapping.

Now, the smoothing using low-pass Gaussian filter is performed as follows (Eq. 23 and Eq. 24):

$$\varphi_x(i,j) = \sum_{u=\frac{-w_\rho}{2}}^{\frac{w_\rho}{2}} \sum_{v=\frac{-w_\rho}{2}}^{\frac{w_\rho}{2}} F(u,v)\Phi_x(i-uw_\rho, j-vw_\rho) \quad (23)$$

$$\varphi_y(i,j) = \sum_{u=\frac{-w_\rho}{2}}^{\frac{w_\rho}{2}} \sum_{v=\frac{-w_\rho}{2}}^{\frac{w_\rho}{2}} F(u,v)\Phi_y(i-uw_\rho, j-vw_\rho) \quad (24)$$

where, $F(u, v)$ is a two-dimensional Gaussian low pass filter and $w\rho$ x $w\rho$ specifies the size of the filter. Finally, the smoothed orientation field O is computed by using the Eq.25,

$$O(i,j) = \frac{1}{2}\tan^{-1}\left[\frac{\varphi_y(i,j)}{\varphi_x(i,j)}\right] \quad (25)$$

Fig. 10 and Fig. 11 shows the orientation field plot for the fingerprint image with and without overlapping with approximate sub-image.

E. Local Ridge Frequency Estimation

In a local neighbourhood where there is no minutiae and singular points appear, the ridge and valley structure can be estimated as a sinusoidal shaped plane wave with constant frequency along the direction normal to the local ridge

orientation. The local ridge frequency *Ω(i,j)* is defined as the frequency of ridge and the valley structure in a local

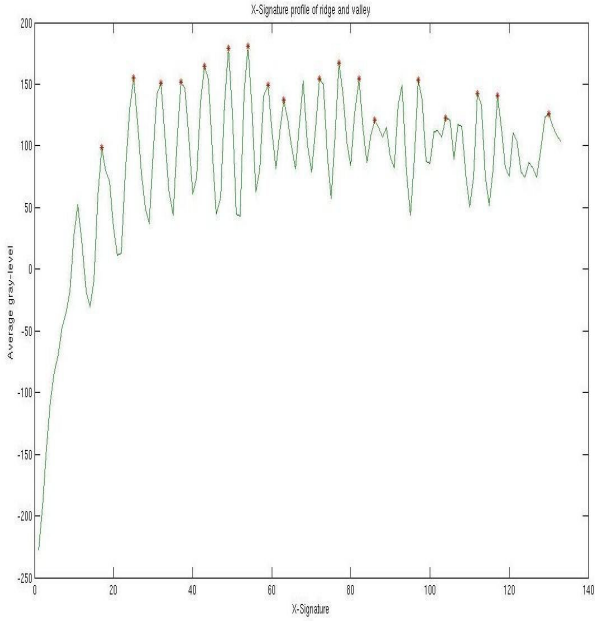

Figure 12. X −Signature profile of fingerprint image.

neighborhood along a direction normal to the local ridge orientation θ_{ij}. [1].

To estimate the local ridge frequency we adopt the X−signature method [5]. The algorithm is as follows:
1) Divide the approximate sub-image *A(i, j)* into block size of $w \times w(8 \times 8)$.
2) For each block centered at pixel *(i, j)* a $l \times w(16 \times 8)$ oriented window is defined in ridge coordinate system (i.e., rotated to align the y-axis with the local ridge orientation).
3) Now, for each block centered at pixel *(i, j)* the X−signature values are calculated. The X−signature of the gray-levels is obtained by accumulating, for each column *X*, the gray-levels of the corresponding pixels in the oriented value. The X−signature value is computed with the help of Eq. 26:

$$X[k] = \frac{1}{w}\sum_{p=0}^{w-1} A(m,n) \qquad k = 0, 1, \ldots, l-1 \tag{26}$$

where, *m* and *n* are the ridge coordinates defined by the Eq. 28 and Eq. 29, respectively

$$m = i + (p - \frac{w}{2})\cos(O(i,j)) + (k - \frac{l}{2})\sin(O(i,j)) \tag{27}$$

$$n = j + (p - \frac{w}{2})\sin(O(i,j)) - (k - \frac{l}{2})\cos(O(i,j)) \tag{28}$$

If there is no minutiae and singular points in the oriented window then the X−signature values forms a sinusoidal waveform and ridge frequency can be determined reliably. If the estimated inter-ridge pitch is outside this range, or if the X−Signature profile does not form a well-defined sinusoidal plane wave, the estimated frequency of the block is rejected.

The ridge frequency *Ω(i, j)* is defined as,

$$\Omega(i,j) = \frac{1}{P(i,j)} \tag{29}$$

where, *P(i, j)* is the average number of pixel between two consecutive peaks in the *X*−signature profile or the average distance between the two consecutive peaks of *X*−signature profile. Since, *S(i, j)* is the average distance between the two consecutive peaks therefore sometimes it can be considered as the ridge wavelength. Fig. 12 shows the *X*−signature profile of the fingerprint image.

For the FBI scanning standard of 500 dpi image this frequency ranges from 3 to 25 pixels per pitch between ridges i.e *[1/25, 1/3]*.

F. Gabor Filtering and Wavelet Reconstruction

The ridges and valleys in the fingerprint image forms a sinusoidal shaped plane wave that vary slowly in a local constant orientation with almost constant frequency. The fingerprint image contains noise that should be removed before doing feature extraction and matching. The configurations of parallel ridges and valleys with well-defined frequency and orientation in a fingerprint image provides useful information which helps in removing undesired noise. Since, gabor filter being a bandpass filter has both orientation-selective and frequency-selective properties and has optimal joint resolution in both spatial and frequency domain therefore, a gabor filter which is a band pass filter tuned to the corresponding frequency and orientation can effectively removes the undesired noise and preserve the ridge-valley structure of the fingerprint image. The even-symmetric Gabor filter has the general form [19]:

$$g(x, y : \omega, f) = exp - \frac{1}{2}(\frac{x_\omega^2}{\sigma_x^2} + \frac{y_\omega^2}{\sigma_y^2})\cos(2\pi f x_\omega) \tag{30}$$

where ω is the orientation of the Gabor filter, f is the frequency of sinusoidal plane wave and σ_x and σ_y are the space constants of the Gaussian envelope in the x and y directions. The x_ω and y_ω are defined by the following equations.

$$x_\omega = x\cos(\omega) + y\sin(\omega) \tag{31}$$

$$y_\omega = -x\sin(\omega) + y\cos(\omega) \tag{32}$$

The modulation transfer function (MTF) of the Gabor filter is defined as:

$$G(u,v:\omega,f) = 2\pi\sigma_x\sigma_y exp-\frac{1}{2}(\frac{(u_\omega-u_0)^2}{\sigma_u^2}+\frac{(v_\omega-v_0)^2}{\sigma_v^2})+ 2\pi\sigma_x\sigma_y exp-\frac{1}{2}(\frac{(u_\omega+u_0)^2}{\sigma_u^2}+\frac{(v_\omega+v_0)^2}{\sigma_v^2})$$

where, u_ω, v_ω, u_0, v_0, σ_u and σ_y are defined as:

$$u_\omega = u\cos(\omega)+v\sin(\omega) \quad (33)$$

$$u_\omega = -u\sin(\omega)+v\cos(\omega) \quad (34)$$

$$u_0 = \frac{2\pi\cos(\omega)}{f} \quad (35)$$

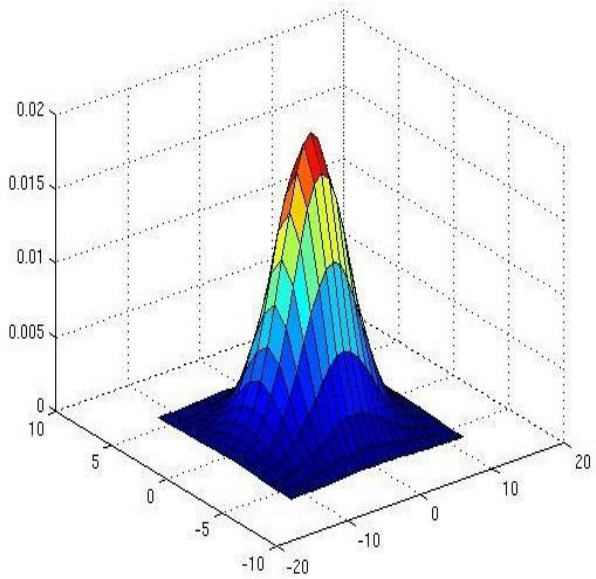

Figure 13. Even-Symmteric Gabor filter with ω=0 and f =10.

$$v_0 = \frac{2\pi\sin(\omega)}{f} \quad (36)$$

$$\sigma_u = \frac{1}{2\pi\sigma_x} \quad (37)$$

$$\sigma_v = \frac{1}{2\pi\sigma_y} \quad (38)$$

The even-symmetric Gabor filter is shown in Fig. 13. To apply Gabor filter to the fingerprint image three parameters must be specified:

1) The filter orientation, ω
2) The frequency, f of the sinusoidal plane wave.
3) The standard deviations (space constants) of the Gaussian kernel, σx and σy

The selection of σx and σy involves a trade-off between robustness and spurious ridges. The smaller values of σx and σy are not effective in noise removal as the resulting image is simply the smoothed version of the original image. On the other hand, the higher values of σx and σy leads to the enhancement artifacts and a significant amount of blurring of the ridge-valley structure. This blurring occurs due to the over smoothing of the image by the Gabor filter. Also, the higher values are more likely to create spurious ridges and valleys than the smaller values of σx and σy. Hong et al [5] empirically set the values of σx and σy to 4.0. S. Greenberg et al [6] set $\sigma^2_x = 4.0$ and $\sigma^2_y = 3.0$. Taking constant values of σx and σy leads to a constant bandwidth, which does not take into account the variation that may occur in the values of ridge frequency. This leads to non-uniform enhancement or enhancement artifacts.

The value of σx determines the degree of contrast enhancement between ridges and valleys whereas, the value of σy determines the amount of smoothing applied to the ridges along the local ridge orientation.

In our algorithm, we have determine the values of σx and σy using the following relation:

$$\sigma_x = m_x f \quad (39)$$

$$\sigma_y = m_y f \quad (40)$$

where, m_x and m_y are constants. The enhanced image of the approximation sub-image is obtained as follows:

$$E(i,j) = \sum_{u=-\frac{w_g}{2}}^{\frac{w_g}{2}} \sum_{v=-\frac{w_g}{2}}^{\frac{w_g}{2}} h(u,v:O(i,j),f)A(i-u,j-v) \quad (41)$$

The detail sub-images not only contain noises, but also include a number of detail information, that cannot be ignore. So, we also perform filtering on detail sub-images before wavelet reconstruction. Let the detail sub-images are *H(i, j), V(i,j)* and *D(I,j)*, respectively. All the detail-sub images are enhanced by reference to the local ridge orientation θ_{ij} of the approximation sub-image. We can compute the enhanced detail sub-images according to Eq. 41 by replacing *A(i − u, j − v)* with *H(i − u, j − v), V (i − u, j − v)* and *D(i − u, j − v),* respectively. Finally, the enhanced fingerprint is obtained by reconstructing the images using 2D discrete inverse wavelet transform.

IV. RESULTS

The purpose of fingerprint image enhancement is to improve the quality of fingerprint images and make them more suitable for minutiae extraction algorithm. In our algorithm, tests are conducted on 500dpi resolution fingerprint image from FVC2002 fingerprint database. The average number of pixels between two consecutive peaks of the *X*–Signature profile comes out to be almost equal to 6. Therefore, the ridge frequency, *f=1/6*, which lies in the standard range specified by FBI for 500dpi resolution images. For filtering the image Gabor filter is tuned to same frequency, *f.*

The selection of the values of σx and σy for Gabor filter is very important as it involves a trade-off between robustness and spurious ridges. In our algorithm, σx and σy are defined by the Eq. 39 and Eq. 40, respectively. To check the trade-off, we have taken m_x = (5.5, 7, 8.5, 13, 20, 25) and m_y = (4, 5, 6, 11, 18, 25). The results of filtering by using different values of m_x and m_y are shown in Fig. 14 to Fig. 19. Results show that on increasing the values of m_x and m_y, more spurious ridges will introduce degarding the quality of fingerprint image. Using m_x = 8.5 and m_y = 6 provides a reasonable trade-off.

V. CONCLUSION

This paper proposes a enhnacement algorithm using gabor filter in wavelet domain. Estimating the local ridge orientation and frequency in wavelet domain can reduce the influence of detail information, so that computed orientation is more accurate. Present algorithm effectively improves the quality of fingerprint image. In a word, a refined gabor filter is applied in fingerprint image processing, then a good quality of fingerprint image is acheived, and the performance of the fingerprint recognition system has been improved.

Figure 14. Filtered image with f=0.16, m_x=5.5 and m_y=4.

Figure 15. Filtered image with f=0.16, m_x=7 and m_y=5.

Figure 16. Filtered image with f=0.16, m_x=8.5 and m_y=6.

Figure 17. Filtered image with f=0.16, m_x=13 and m_y=11.

Figure 18. Filtered image with f=0.16, m_x=20 and m_y=18

Figure 19. Filtered image with f=0.16, m_x=25 and m_y=25

ACKNOWLEDGMENT

We gratefully acknowledge our many useful discussions with our guide Dr. Vipan Kakar.

REFERENCES

[1] Davide Maltoni, Dario Maio, Anil K. Jain, Salil Prabhakar, *HandBook of Fingerprint Recognition*, Second Edition, Springer-Verlag (2009).

[2] F. Galton, Finger Prints, London: Macmillan (1892).

[3] American National Standards Institute, Fingerprint Identification-Data Format for Information Interchange. New York, 1986.

[4] A. Jain, L. Hong, and R. Bolle, "On-Line Fingerprint Verification", *IEEE Transaction on Pattern and Machine Intelligence* 19(4), 302-314 (1997)

[5] Lin Hong, Yifei Wan and A. Jain, "Fingerprint Image Enhancement:Algorithm and Performance Evaluation", *IEEE Transaction on Pattern Analysis and Machine Intelligence* 20(8), 777-789 (1998).

[6] Shlomo Greenberg, Mayer Aladjem and Daniel Kogan, "Fingerprint Image Enhancement using Filtering Techniques", *Real Time Imaging* 8, 227-236 (2002).

[7] A. Jain, S. Prabhakar and S. Pankanti, "*Matching and Classification: A Case Study in Fingerprint Domain* " PINSA 67(2), 223-241 (2001).

[8] A.M. Paul, and R.M. Lourde, "A Study on Image Enhancement Techniques for Fingerprint Identification" in *Proceedings of the IEEE International Conference on Video and Signal Based Surveillance* (2006).

[9] Jianwei Yang, Lifeng Liu, Tianzi Jiang, and Yong Fan, "A modified Gabor filter design method for fingerprint image enhancement," *Pattern Recognition Letters* 24, 1805-1817 (2003).

[10] Miao-li Wen, Yan Liang, Quan Pan, and Hong-cai Zhang, "A Gabor Filter Based Fingerprint Enhancement Algorithm in Wavelet Domain" in *Proceedings of Internationa Symposium on Communication and Information Technologies*, 1421-1424 (2005).

[11] Wei Wang, Jianwei Li, Feifei Huang, and Hailiang Feng, "Design and implementation of Log-Gabor filter in fingerprint image enhancement" *Pattern Recognition Letters* 29(3), 301-308 (2008).

[12] Fu Bo, Han Zhi, and Li Zheng, "A Novel Fingerprint Enhancement Method Based on Gabor Filtering" in 2ndInternational Congress on Image and Signal Processing,(CISP09), 1-5 (2009).

[13] Safar Hatami, Reshad Hosseini, Mahmoud Kamarei, and Hossein Ah-madi, "Wavelet Based Fingerprint Image Enhancement" in International Symposium on Circuits and Systems, 4610-4613 (2005).

[14] Heikki Ailisto, Mikko Lindholm, and Pauli Tikkanen, "A Review of Fingerprint Image Enhancement Methods" *International Journal of Image and Graphics* 3(3), 401-424 (2003).

[15] S.G. Mallat, "*A Wavelet Tour of Signal Processing*" Second Edition, Academic Press (1999).

[16] R.C. Gonzalez, and R.E. Woods, "*Digital Image Processing*", Third Edition, Prentice-Hall India (2008).

[17] S. G. Mallat, "A theory for multiresolution signal decomposition: the wavelet representation" *IEEE Transaction on Pattern Analysis and Machine Intelligence* 11(7), 674-693 (1989).

[18] M. S. Helfroush, and M. Mohammadpour, "Fingerprint Segmentation" *World Applied Sciences Journal* 6(3), 303-308 (2009).

[19] J. R. Movellan "*Tutorial on Gabor Filters*", 2008.